AIP | Applied Physics Letters

Measurement of bi-directional ion acceleration along a convergent-divergent magnetic nozzle

Yunchao Zhang, Christine Charles, and Rod Boswell

Citation: Applied Physics Letters **108**, 104101 (2016); doi: 10.1063/1.4943583
View online: http://dx.doi.org/10.1063/1.4943583
View Table of Contents: http://scitation.aip.org/content/aip/journal/apl/108/10?ver=pdfcov
Published by the AIP Publishing

Measurement of bi-directional ion acceleration along a convergent-divergent magnetic nozzle

Yunchao Zhang,[a] Christine Charles, and Rod Boswell
Space Plasma, Power and Propulsion Laboratory, Research School of Physics and Engineering, The Australian National University, Bldg. 60, Mills Road, Australian Capital Territory 2601, Australia

(Received 8 January 2016; accepted 26 February 2016; published online 7 March 2016)

Bi-directional plasma expansion resulting in the formation of ion beams travelling in opposite directions is respectively measured in the converging and diverging parts of a magnetic nozzle created using a low-pressure helicon radio-frequency plasma source. The axial profile of ion saturation current along the nozzle is closely correlated to that of the magnetic flux density, and the ion "swarm" has a zero convective velocity at the magnetic throat where plasma generation is localized, thereby balancing the bi-directional particle loss. The ion beam potentials measured on both sides of the magnetic nozzle show results consistent with the maximum plasma potential measured at the throat. © *2016 AIP Publishing LLC*. [http://dx.doi.org/10.1063/1.4943583]

Ion acceleration along a magnetic field plays an important role in physical systems spanning astro-physical phenomena[1] down to electric propulsion systems for spacecrafts[2,3] and plasma processing for semiconductors.[4] In these low pressure plasmas, the light electrons are approximately in equilibrium due to their large thermal velocity, while the heavy ions are not and their motion is greatly affected by the electron pressure via the electric field.[5,6] As a magnetic field confines charged particles across its perpendicular direction and guides their fluxes along the parallel direction which functions like a nozzle[7,8] and the pressure-determined momentum performance of an ion swarm is similar to a compressible gas flow, ion acceleration along a convergent-divergent magnetic field has been previously studied as a classic uni-directional nozzle flow.[9,10] Numerous studies have investigated factors that influence ion acceleration, including double layer,[11–13] gas types,[14] and neutral depletion.[15,16] The present study focuses on an experimental observation of bi-directional ion acceleration along a convergent-divergent magnetic nozzle with a zero convective velocity at the magnetic throat.

The experiment is carried out in the Chi-Kung reactor as shown in Figure 1(a), which, on the left hand side ($z < 0$ cm), consists of a cylindrical plasma source terminated with an aluminium earthed plate and, on the right hand side ($z > 0$ cm), a contiguously attached 30-cm long, 32-cm diameter, earthed aluminium diffusion chamber. The plasma source is made of a 31-cm long, 13.7-cm inner diameter, 0.65-cm thick Pyrex glass tube, and surrounded by an 18-cm long double saddle antenna operating at a constant power of 310 W at a radio frequency (RF) of 13.56 MHz. A solenoid close to the source exit is used to generate a convergent-divergent magnetic nozzle whose field lines are calculated from the Biot-Savart law and shown in Figure 1(a) as solid curves. A turbo/primary pumping system is implemented to obtain a base pressure of 4.5×10^{-6} Torr in the reactor monitored with an ion gauge. Argon gas is fed to the system through a side wall port of the diffusion chamber at a constant gas pressure of 5.0×10^{-4} Torr measured with a Baratron gauge.

Four electrostatic probes are used as experimental diagnostics: a Langmuir probe (LP), an emissive probe (EP), and two retarding field energy analysers (RFEAs), with their probe shafts and the reactor walls being grounded. A vacuum slide is mounted on the back plate of the diffusion chamber to allow positioning of the probes along both the axial and radial directions without breaking vacuum (except when changing the probe). The LP has a 1.9-mm diameter nickel tip and measures the ion saturation current at a negative bias voltage of −95 V. The EP consisting of a 0.2-mm diameter tungsten wire measures the plasma potential using the floating potential method. The RFEA, previously described in detail in Ref. 17, comprises of a structure with a 2-mm diameter orifice, four grids (an earthed grid, a repellor grid biased at −80 V, a discriminator grid, and a secondary suppressor grid at −18 V), and a collector plate biased at −9 V. It measures the characteristic current-voltage curve $I_c(V_d)$ by sweeping the discriminator voltage from 0 V to 80 V and measuring the corresponding collector current. The first derivative of $I_c(V_d)$ curve represents the ion energy distribution function (IEDF), which can be used to: (1) detect the

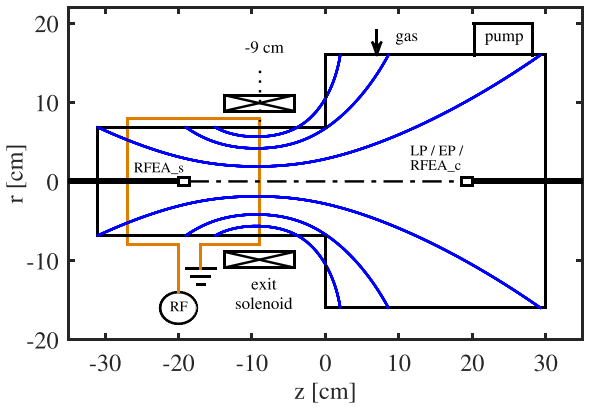

FIG. 1. Chi-Kung reactor implemented with a convergent-divergent magnetic nozzle, showing the major components and diagnostic probes. The calculated field lines are plotted within the reactor geometry.

[a]yunchao.zhang@anu.edu.au

presence of an ion beam (IEDF exhibiting two peaks) or the absence of an ion beam (single-peak IEDF), and (2) derive the direct-current components of local plasma potential (V_p) and ion beam potential (V_b, if an ion beam is present). Here, any sheath oscillation in front of the earthed RFEA[17] simply results in some peak broadening (as confirmed by the consistency between the RFEA and EP measurement of potentials).

For the present experiment, a current of 9 A generated from the direct-current (DC) power supply is transmitted into the double-coil-wound solenoid, i.e., a current of 4.5 A in each coil, and this setting is used by default unless otherwise specified. The magnetic flux density (where $B_z = B$) on the central axis ranging from $z = -25$ cm to 10 cm, is measured by a gaussmeter. The data, represented by open squares scaled with the right labelled y-axis in Figure 2(a), show a maximum of 200 Gauss at $z = -9$ cm (i.e., location of the magnetic throat) and a symmetric decrease to tens of Gauss in the top region of the plasma source and in the diffusion chamber. Calculated results from the Biot-Savart law are given by the solid line and are consistent with the measurements.

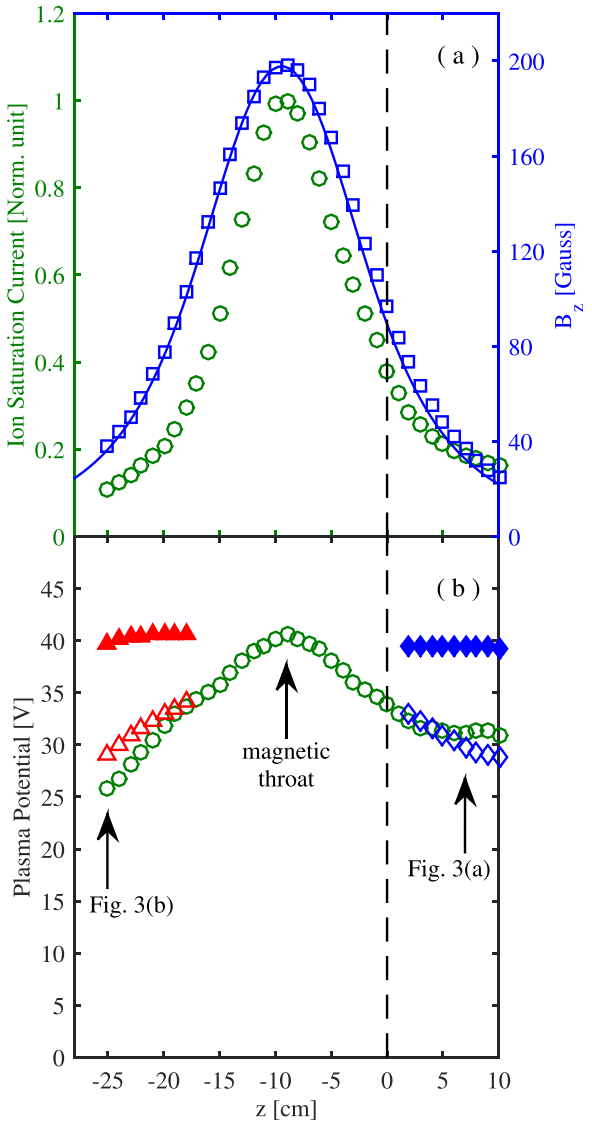

FIG. 2. (a) Right labelled y-axis: On-axis magnetic flux density generated by a current of 9 A supplied into the solenoid, measured using a gaussmeter (◯) and calculated by the Biot-Savart law (solid line). Left labelled y-axis: axial profile of normalized ion saturation current measured by the LP (◯). (b) Axial profiles of plasma potential measured by the EP (◯), beam potential obtained by RFEA_c (◆) and RFEA_s (▲), and plasma potential obtained by RFEA_c (◇) and RFEA_s (△). The vertical dashed line show the location of source-chamber interface at $z = 0$ cm.

The normalized ion saturation current, represented by open circles scaled with the left labelled y-axis in Figure 2(a), follows a similar profile to that of the magnetic flux density with a maximum at the magnetic throat ($z = -9$ cm). This configuration is similar to that generated in previous experimental studies of electrode-less Helicon thrusters,[6,18] where the maximum ion saturation current corresponds to the location of plasma generation, which is further verified by measuring the axial plasma potential profile using the EP, represented by open circles in Figure 2(b): a peak value of about 40 V is measured at $z = -9$ cm and decreases along both axial directions; the larger potential decrease of ~10 V measured from $z = -15$ cm to -25 cm compared to ~5 V from $z = -3$ cm to 10 cm results from the closer proximity of the grounded source end plate at $z = -31$ cm.

In order to fully characterize ion transport and acceleration along both directions of the magnetic nozzle, two RFEAs are positioned face-to-face: one RFEA is mounted through the vacuum slide into the diffusion chamber with its orifice facing the plasma source (Figure 1(a)), denoted as "RFEA_c," and the second RFEA is inserted via the top aluminium grounded plate terminating the plasma source with its orifice facing the diffusion chamber, denoted as "RFEA_s." Under the present experimental condition, the placement of RFEA_c in the axial range of $z > 2$ cm or RFEA_s in the range of $z < -18$ cm has a negligible perturbation (less than a few percent) on plasma parameters, determined by moving one RFEA on axis and using the other one as a witness probe. For these regions, the local plasma potential measured by the RFEAs show similar results to those obtained by the EP, with a maximum deviation of about 3 V and an ion beam is simultaneously detected by both RFEAs: the beam potential values measured by RFEA_s in the range from $z = -25$ cm to -18 cm in the plasma source, represented by solid triangles in Figure 2(b), and those measured by RFEA_c from $z = 2$ cm to $z = 10$ cm in the diffusion chamber, represented by solid diamonds, are in very good agreement with the EP-measured maximum plasma potential at the magnetic throat ($z = -9$ cm). Other high-field experiments[6] have also shown that the plasma density and potential profiles are defined by the magnetic flux density profile.

These results provide clear evidence that bi-directional ion acceleration is present where an ion beam, with a zero convective velocity at the magnetic throat, is formed and simultaneously travels "forward" into the diffusion chamber and "backward" in the closed region of the plasma source. Examples of the IEDF curves obtained by RFEA_c at $z = 7$ cm in the diffusion chamber and by RFEA_s at $z = -25$ cm in the plasma source (both locations being 16 cm away from the magnetic throat as indicated in Figure 2(b)) are shown as solid lines in Figures 3(a) and 3(b) and present a similar two-peak distribution with a beam potential value of about 40 V. The ion beam energy at those positions is about 10 eV. This confirms that the plasma generation due to ionization must be localized in the throat region of the magnetic nozzle to supplement this bi-directional particle loss carried by the ion

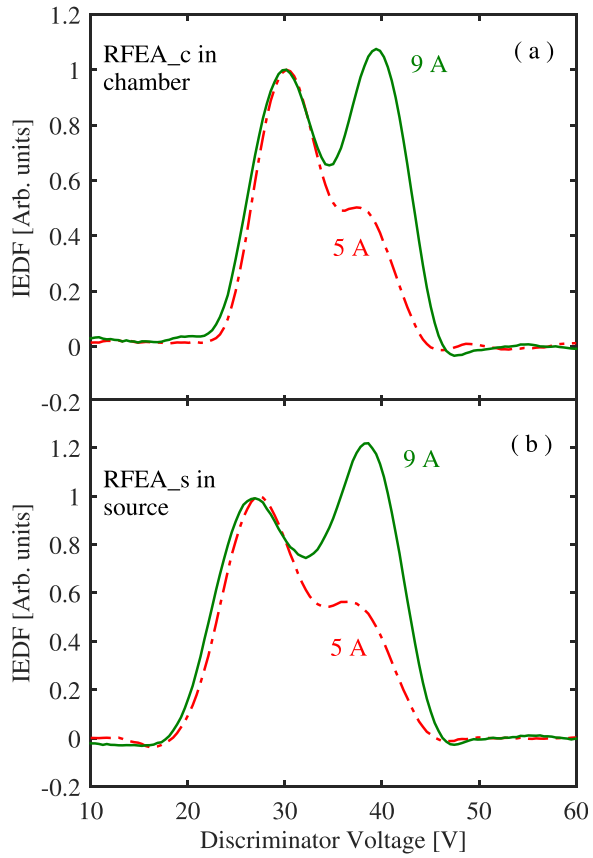

FIG. 3. IEDFs obtained by (a) RFEA_c at $z = 7$ cm in the diffusion chamber and (b) RFEA_s at $z = -25$ cm in the plasma source, for current values of 9A (solid line) and 5A (dashed-dotted line) supplied into the solenoid.

beam. Details of the ionization mechanism are beyond the scope of this study and it is simply noted that the magnetic field intensity influences the ion beam strength as shown by the IEDF measurements (represented by dashed-dotted lines) at both RFEA locations with a smaller current of 5 A supplied into the solenoid: a two-peak IEDF is still observed where the beam potential is unchanged (compared to the case of 9 A) as previously observed in similar systems,[19] but exhibits a lower magnitude at the beam potential. Additional measurements (not given in Figure 3) show that the solenoid has a minimum threshold current of about 4 A for stable ion beam condition as observed in other experiments with different geometries.[20]

The experimental nozzle configuration is not fully "symmetric" due to the geometric expansion (at $z = 0$ cm) marked by the vertical dashed line in Figure 2. To illustrate this, the radial profiles of normalized ion saturation current at $z = -2$ cm in the source-exit region and at $z = -17$ cm in the source-top region are shown in Figures 4(a) and 4(b), respectively. Both profiles are symmetric around the central axis, but a single-peak profile is observed in the exit region likely due to plasma expansion from the source-chamber interface into the diffusion chamber. These results confirm that additional radial and azimuthal effects need to be considered when analysing the momentum behavior in a magnetic nozzle.[5,6]

Plasma dynamics in a magnetic nozzle can be greatly affected by details of ionization. Ion "swarm" acceleration along one direction of the nozzle similarly to a compressible

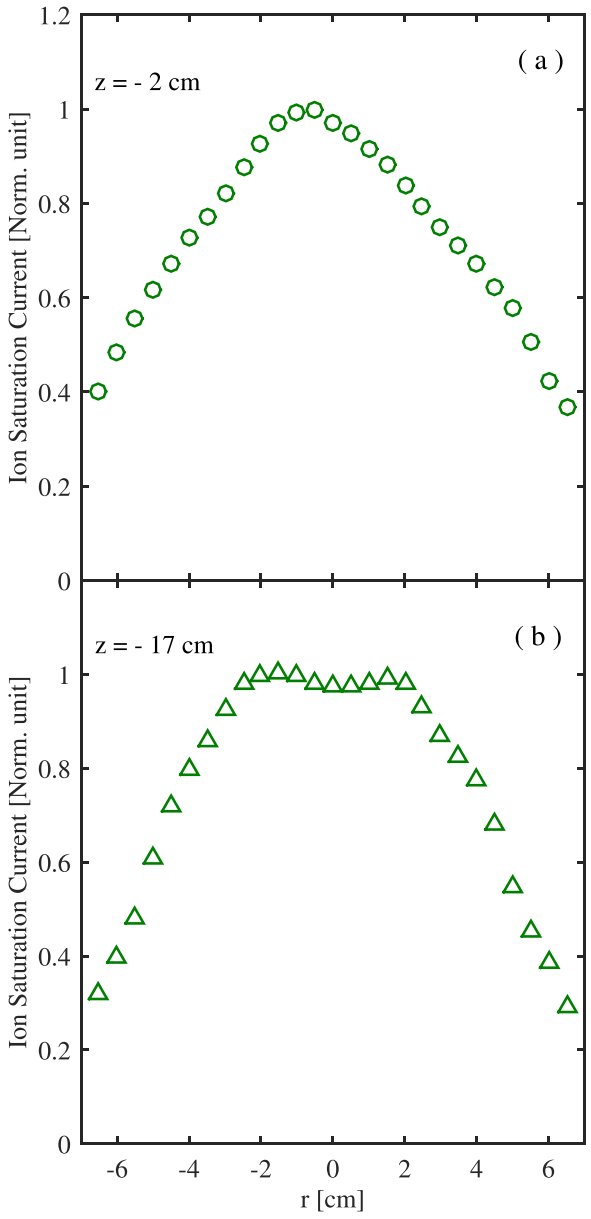

FIG. 4. Radial profiles of normalized ion saturation current measured by the LP at, (a) $z = -2$ cm in the source-exit region (◯) and (b) $z = -17$ cm in the source-top region (△).

gas flow in a Laval nozzle has been described.[7–10] By using a one-dimensional fluidic approach to describe a fully magnetized plasma expansion along a magnetic nozzle, Fruchtman[21] predicted that ionization (acting as a mass addition term to the nozzle equation) could cause bi-directional ion fluxes. In the simple case of no magnetic field, ionization is the source of free-fall ions moving along decreasing potentials as detailed by Tonks and Langmuir.[22] Here, we show the direct experimental evidence of bi-directional ion acceleration along a magnetic nozzle, a result of localized plasma generation in the magnetic throat region. Interestingly, the present plasma source configuration generating bi-directional ion acceleration could provide a compact and simplified system for deorbiting space debris where one ion beam targets the space debris and the opposite ion beam prevents spacecraft drift. A few studies on the "ion beam shepherd" technique involving two plasma propulsion systems implemented onto the spacecraft have

been recently conceptually described[23,24] in the active field of space debris mitigation.

In summary, this experimental study shows experimental evidence of bi-directional ion acceleration along the axis of a convergent-divergent magnetic nozzle in a low pressure laboratory plasma. The ion beam has a zero convective velocity at the magnetic throat where localized plasma generation occurs to balance the bi-directional particle loss. Its strength is positively correlated to the magnetic field intensity.

[1]E. N. Parker, *Cosmical Magnetic Fields: Their Origin and Their Activity, International Series of Monographs on Physics* (Oxford University Press, New York, 1979).

[2]D. M. Goebel and I. Katz, *Fundamentals of Electric Propulsion: Ion and Hall Thrusters, JPL Space Science and Technology Series* (John Wiley & Sons, New York, 2008).

[3]C. Charles, R. W. Boswell, and K. Takahashi, "Boltzmann expansion in a radiofrequency conical helicon thruster operating in xenon and argon," Appl. Phys. Lett. **102**, 223510 (2013).

[4]M. A. Lieberman and A. J. Lichtenberg, *Principles of Plasma Discharges and Materials Processing*, 2nd ed. (John Wiley & Sons, New York, 2005).

[5]A. Fruchtman, K. Takahashi, C. Charles, and R. W. Boswell, "A magnetic nozzle calculation of the force on a plasma," Phys. Plasmas **19**, 033507 (2012).

[6]K. Takahashi, T. Lafleur, C. Charles, P. Alexander, and R. W. Boswell, "Electron diamagnetic effect on axial force in an expanding plasma: Experiments and theory," Phys. Rev. Lett. **107**, 235001 (2011).

[7]W. M. Manheimer and R. F. Fernsler, "Plasma acceleration by area expansion," IEEE Trans. Plasma Sci. **29**, 75 (2001).

[8]A. V. Arefiev and B. N. Breizman, "Ambipolar acceleration of ions in a magnetic nozzle," Phys. Plasmas **15**, 042109 (2008).

[9]C. A. Deline, R. D. Bengtson, B. N. Breizman, M. R. Tushentsov, J. E. Jones, D. G. Chavers, C. C. Dobson, and B. M. Schuettpelz, "Plume detachment from a magnetic nozzle," Phys. Plasmas **16**, 033502 (2009).

[10]B. W. Longmier, E. A. B. III, M. D. Carter, L. D. Cassady, W. J. Chancery, F. R. C. Díaz, T. W. Glover, N. Hershkowitz, A. V. Ilin, G. E. McCaskill, C. S. Olsen, and J. P. Squire, "Ambipolar ion acceleration in an expanding magnetic nozzle," Plasma Sources Sci. Technol. **20**, 015007 (2011).

[11]C. Charles and R. W. Boswell, "Current-free double-layer formation in a high-density helicon discharge," Appl. Phys. Lett. **82**, 1356 (2003).

[12]X. Sun, A. M. Keesee, C. Biloiu, E. E. Scime, A. Meige, C. Charles, and R. W. Boswell, "Observations of ion-beam formation in a current-free double layer," Phys. Rev. Lett. **95**, 025004 (2005).

[13]O. Sutherland, C. Charles, N. Plihon, and R. Boswell, "Experimental evidence of a double layer in a large volume helicon reactor," Phys. Rev. Lett. **95**, 205002 (2005).

[14]N. Plihon, P. Chabert, and C. S. Corr, "Experimental investigation of double layers in expanding plasmas," Phys. Plasmas **14**, 013506 (2007).

[15]A. W. Degeling, T. E. Sheridan, and R. W. Boswell, "Intense on-axis plasma production and associated relaxation oscillations in a large volume helicon source," Phys. Plasmas **6**, 3664 (1999).

[16]A. Fruchtman, G. Makrinich, P. Chabert, and J. M. Rax, "Enhanced plasma transport due to neutral depletion," Phys. Rev. Lett. **95**, 115002 (2005).

[17]C. Charles and R. W. Boswell, "Laboratory evidence of a supersonic ion beam generated by a current-free helicon double-layer," Phys. Plasmas **11**, 1706 (2004).

[18]Y. Zhang, C. Charles, and R. W. Boswell, "Transport of ion beam in an annular magnetically expanding helicon double layer thruster," Phys. Plasmas **21**, 063511 (2014).

[19]C. Charles and R. W. Boswell, "The magnetic-field-induced transition from an expanding plasma to a double layer containing expanding plasma," Appl. Phys. Lett. **91**, 201505 (2007).

[20]K. Takahashi, C. Charles, R. W. Boswell, and T. Fujiwara, "Double-layer ion acceleration triggered by ion magnetization in expanding radiofrequency plasma sources," Appl. Phys. Lett. **97**, 141503 (2010).

[21]A. Fruchtman, "Electric field in a double layer and the imparted momentum," Phys. Rev. Lett. **96**, 065002 (2006).

[22]L. Tonks and I. Langmuir, "A general theory of the plasma of an arc," Phys. Rev. **34**, 876 (1929).

[23]C. Bombardelli and J. Peláez, "Ion beam shepherd for contactless space debris removal," J. Guid. Control Dyn. **34**, 916 (2011).

[24]S. Kitamura, Y. Hayakawa, and S. Kawamoto, "A reorbiter for large geo debris objects using ion beam irradiation," Acta Astronaut. **94**, 725 (2014).